Dear Reviewer,

Thank you for your time and constructive comments. We have carefully revised the manuscript accordingly. Below we provide a point-by-point response.

### 1) Emphasis on Problem-Solving in Abstract/Introduction

#### Comment:

The abstract highlighted targeted improvements in: (i) shallow-to-medium layer exploration accuracy, (ii) human–machine interaction complexity, and (iii) constrained data transmission. Suggest strengthening comparative analysis in the main text.

#### Response:

We sincerely appreciate the reviewer's constructive suggestion regarding the comparative analysis. In response, we have strengthened the comparison between our system and commercial instruments in the main text by incorporating the following clarifications:

# i) Shallow-to-medium layer exploration accuracy (Section 1):

We added explanatory text highlighting that our instrument can acquire signals at frequencies up to 1 MHz, whereas commercial instruments (e.g., EH4) are limited to 100 kHz. According to the CSAMT (Controlled Source Audio-frequency Magnetotelluric) methodology, this extended frequency acquisition capability enables our system to achieve enhanced resolution for shallow subsurface structures, thereby addressing the targeted improvement in shallow-to-medium layer exploration mentioned in the abstract.

#### ii) Human-machine interaction complexity (Section 6):

We supplemented the text with comparative observations from field testing. Specifically, we noted that the EH4 commercial system only displays apparent resistivity and phase diagrams without real-time waveform visualization capabilities or raw channel data export functionality. Furthermore, neither the V8 nor EH4 systems incorporate blind acquisition mode, resulting in substantially increased operational time during repetitive multi-station surveys. These limitations contrast with our system's simplified and intuitive operation interface and automated acquisition features, validating the interaction complexity improvements cited in the abstract.

### iii) Constrained data transmission (Section 5):

We added descriptive text confirming that throughout extensive field testing, our instrument exhibited no data stuttering or packet loss during high-speed data transmission and storage operations. This empirical validation demonstrates the feasibility and robustness of our designed data transmission architecture under various field conditions.

### 2) Clarify Field Test Configuration

#### Comment:

Provide detailed descriptions of the 242 measurement points (distribution, geophysical parameters). Enhance Figure 15 by including physical images of EH4 instruments for direct comparison.

### Response:

Thank you so much for your comment. Brief information regarding the 242 measurement points was presented in the original manuscript. Herein, supplementary details of the measurement points and testing procedure are provided as follows:

Each survey line has a length of 3 km, with an interval of 200 m between the two parallel survey lines. A total of 242 measurement points were deployed, with an adjacent point spacing of 25 m; each survey line contains 121 measurement points. The layout of field test stations is illustrated in Figure 14.

The transmission module comprises a high-frequency transmitter and a low-frequency transmitter. The low-frequency transmitter was positioned 8 km away from the vertical survey lines; preliminary tests verified that its transmitted signals could cover both survey lines, thus its position was maintained unchanged throughout the entire testing process. In contrast, the high-frequency transmitter was placed 200 m away from the survey lines. As confirmed by tests, the high-frequency signals can cover 7 measurement points (e.g., when the transmitter is situated at the LS05-105 measurement point, its transmitted signals can cover the range from LS03-99 to LS03-111). Therefore, the high-frequency transmitter was moved synchronously with the receiver to ensure that the receiver remained within the coverage of the transmitted signals. During the testing process, the station layout at each measurement point was consistent with the receiver layout diagram depicted in Figure 14.

Figure 15 has been updated; the revised field test photographs include the CSUMT-R, EH4, and V8 instruments for visual comparison.

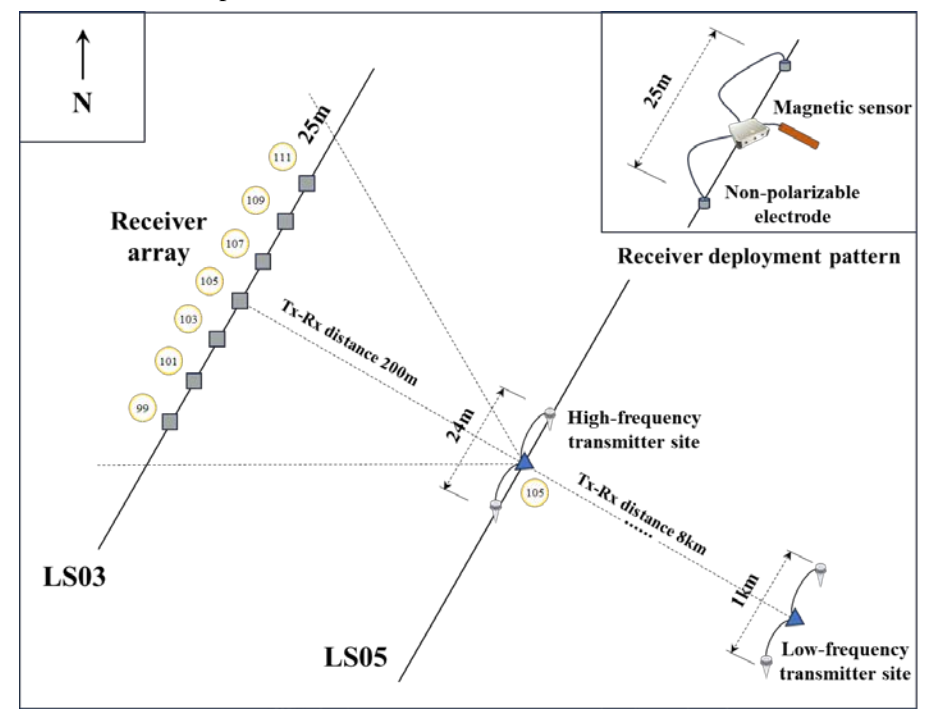


Figure 14. Field station layout in Fengtai ore cluster.



Figure 15. Field test photos in Fengtai ore cluster.

### 3) Validation of Formula 4 (Mean Square Relative Error)

#### Comment:

Clarify whether the metric is industry-standard; cite authoritative sources or explain rationale if novel. Provide contextual validation.

### Response:

We appreciate you raising this point. This formula, designed to assess the consistency of two or more receivers, is derived from *Technical Specification for Controlled-Source Audio-Frequency Magnetotellurics* (Standard No.: **DZ/T 0280-2015**)—a national technical standard widely recognized in the Chinese geophysical exploration industry. As stipulated in this standard, prior to initiating fieldwork in the same survey area, a consistency verification test must be conducted for two or more receivers of the same model. The key requirements of this test are specified as follows: a) The consistency verification of instruments shall be performed under actual field conditions. A site with minimal electromagnetic interference shall be selected to conduct single-point, full-frequency-band measurements.

b) The consistency of the instruments shall be quantified using the total mean square relative error  $\varepsilon$  of the Cagniard resistivity, as observed by m instruments at a given measurement point. The calculation formula specified in the standard is:

$$\varepsilon = \pm \sqrt{\sum_{i=1}^{n} \sum_{j=1}^{m} V_{ij}^{2} / (L - n)}$$

Where  $V_{ij}$  denotes the relative error between the Cagniard resistivity value observed by the j-th instrument at the i-th frequency point and the average Cagniard resistivity value of m instruments at the i-th frequency point; mrepresents the number of instruments involved in the consistency verification test; L is the total count of relative errors  $V_{ij}$ , with  $L = m \times n$ ; n stands for the number of observation frequency points included in the consistency verification test.

The formula employed in this paper is a simplified version of the aforementioned standard formula, with the simplification process ensuring no loss of calculation accuracy for the specific application

scenario of this study.

# 4) Robustness of Instrument Comparison

### Comment:

Figure 17 shows results from a single commercial instrument. Add 1–2 additional instruments (e.g., V8, EH4) to enhance statistical credibility.

# Response:

We have revised Figure 17. The updated figure now includes apparent resistivity plots and phase plots showing the comparisons between CSUMT-R and EH4, as well as between CSUMT-R and V8. Additionally, it incorporates a full-frequency-band comparison plot.

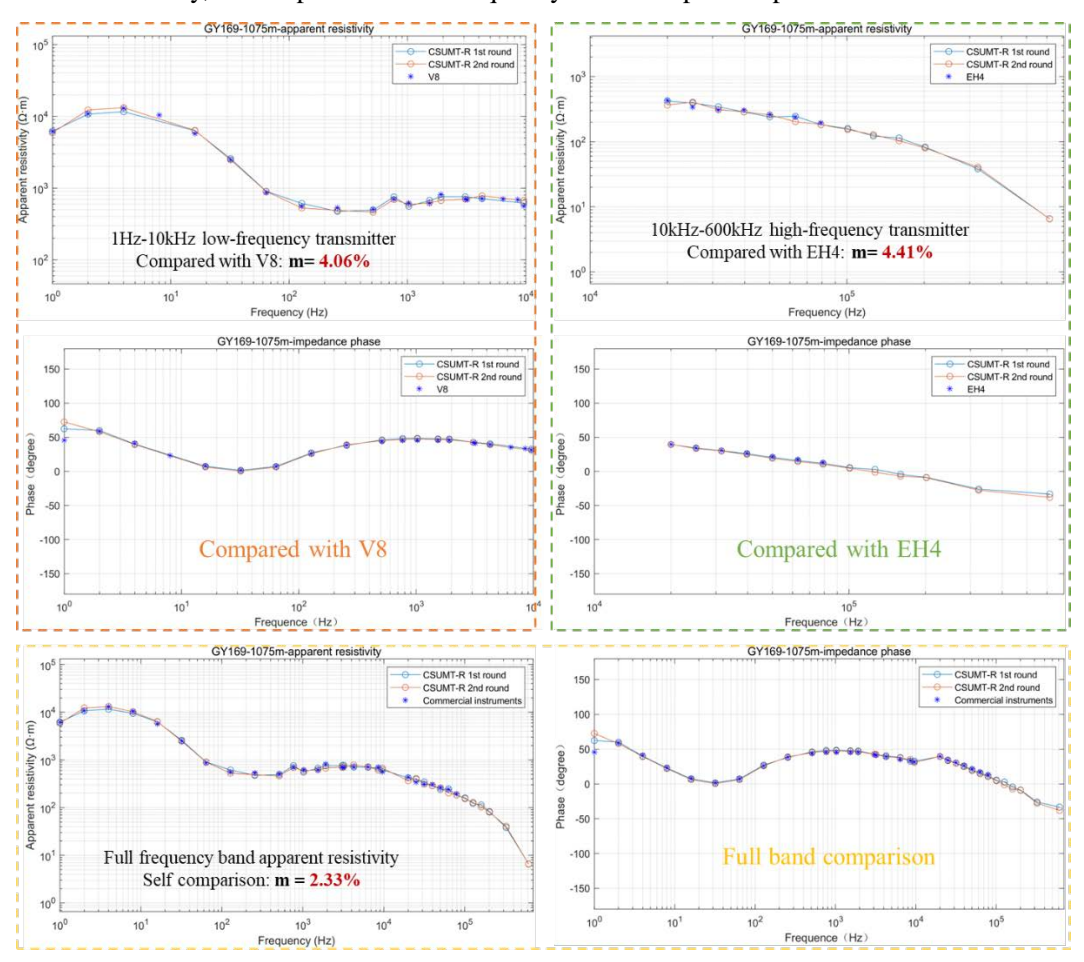


Figure 17. Field data for apparent resistivity and impedance phase for the CSUMT-R and commercial instruments.

### **Future Recommendations**

# 1) Enhanced Field Resilience (BeiDou Satellite Messaging)

Comment:

Integrate BeiDou satellite messaging for data transmission in remote/extreme environments.

Response:

We thank the reviewer for this insightful suggestion. We have recognized the significant potential of BeiDou satellite messaging for data transmission under challenging field conditions, particularly in remote areas with limited conventional communication infrastructure. The integration of BeiDou satellite communication capabilities into our system is currently under active investigation.

### 2) Long-Term Reliability Testing

### Comment:

Include 6–12 month unattended operation data to assess sustained reliability.

#### Response:

We sincerely appreciate the reviewer's emphasis on long-term reliability assessment, which is crucial for field geophysical instrumentation. In response to this suggestion, we have conducted comprehensive reliability testing of our system. From April 2025 to October 2025, field tests were performed in Shaanxi Province, China. During this 6-month deployment period, the system successfully completed a rigorous 3,000-hour fault-free operation test under various environmental conditions, including temperature fluctuations, humidity variations, and electromagnetic interference. This extended reliability testing has been independently verified and certified by a third-party testing institution, confirming the system's sustained operational stability and robustness.

# 3) Methodological Expansion (MT, IP)

#### Comment:

Extend applicability to MT (deep imaging) and IP (mineral exploration).

### Response:

We thank the reviewer for highlighting the importance of methodological versatility. We would like to clarify that our current system already supports magnetotelluric (MT) functionality, including real-time waveform visualization, time-series data processing, and the generation of apparent resistivity and phase pseudosections along survey profiles. These capabilities enable effective deep subsurface imaging applications. Regarding induced polarization (IP) methods for mineral exploration applications, we fully acknowledge their significance and plan to extend our research to encompass IP and other geophysical techniques in future work. This expansion will require additional hardware modifications and algorithm development, which are scheduled as part of our ongoing research program.